

# Nano-Sized Silica Particles for Chemical Mechanical Polishing – Separation, Size Measurement and Determination of the Surface Charge Using Electrical Asymmetrical Flow Field-Flow Fractionation

## General Information

ID0012

<b>Application Technology Info</b>	Chemical Mechanical Polishing (CMP), Silicon Dioxide, Semiconductor EAF4-MALS Postnova EAF2000, PN3621 MALS
<b>Keywords</b>	Electrical Asymmetrical Flow Field-Flow Fractionation, Size Distribution, Surface Charge, CMP

## Introduction

Silica particles in the nano-size range are widely used in many applications including in foodstuffs (as E551 food additive) or personal care products, but also as abrasive in Chemical Mechanical Polishing (CMP) to achieve a precise level of surface smoothness for applications such as semiconductors. In these applications the determination of accurate particle size and particle size distribution is very important [1,2], but also precise knowledge of the surface charge is crucial as it may predict the stability of a suspension or a slurry against unwanted agglomeration or aggregation.

Electrical Asymmetrical Flow Field-Flow Fractionation (EAF4) coupled to Multi-Angle Light Scattering (MALS) detection allows the separation of different particle sizes while enabling access to particle size, electrophoretic mobility and zeta potential of the particles. The separation principle of the EAF4 is shown schematically in Figure 1:

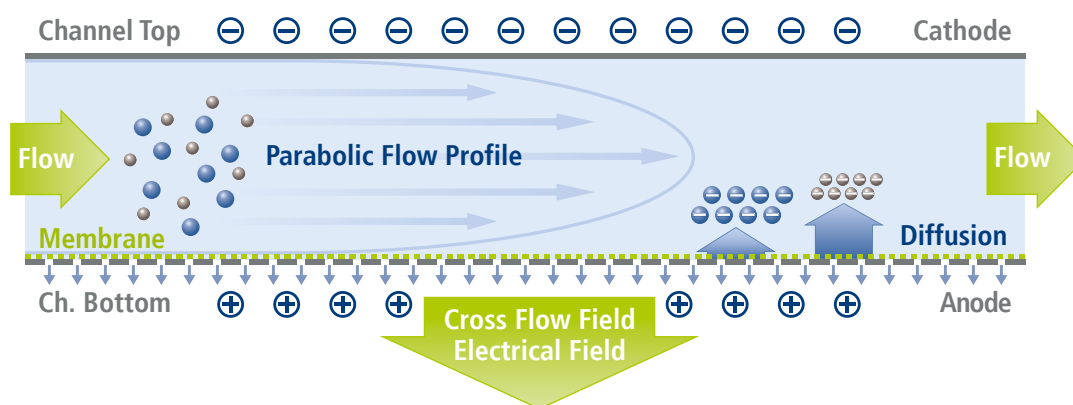


Figure 1: Schematic representation of an Electrical Asymmetrical Flow FFF channel.

## Experimental Details and Results

The material studied in this application note was a bimodal size distribution silicon dioxide sample; the diameter of one fraction was measured at 264 nm and the other fraction at 460 nm by Scanning Electron Microscopy (SEM) analysis. The sample was separated by EAF4 using five different electric field conditions enabling measurement of the electrophoretic mobility and thus the surface zeta potential of both particle fractions. Coupled in line with the EAF4 was a MALS detector to provide simultaneous size determination.

Figure 2 displays the EAF4-MALS fractograms at different electric field conditions which resulted in different retention times. The dotted lines show the radius of gyration ( $R_g$ ) obtained from MALS indicating that the electric field had no influence on the particle size (Table 1). The  $R_g$  results agree very well with the SEM sizes reported for the sample. In the first fractogram (dark blue) separation was achieved solely by the cross flow field without application of an electric field (0 mA). In this case the particles were separated by the difference in their diffusion behavior due to the cross flow perpendicular to the channel flow, which means the particles eluted according to their hydrodynamic size. There are two clearly separated MALS signals for the two size fractions in the sample at approximately 26 and 36 minutes.

The further fractograms in Figure 2 (red, light blue, black and purple) show the same separation with increasing electric fields applied (0.5 mA – 2.0 mA). It can be clearly seen that the electric field induced a measurable shift in the retention time due to the surface charge of the silica particles. This is due to the attractive interactions between the positively charged channel bottom and the negatively charged particles that drag the particles closer to the membrane into slower stream lines of the parabolic channel flow so that they elute at later retention times. By measuring the shift in retention time and relating it to the applied electric field, the electrophoretic mobility and the zeta potential of the particles can be calculated (Figure 3). It is important to note that, unlike batch Zeta potential measurements, the separation ability of EAF4 allows the individual determination of the zeta potential of each of the two size fractions in the sample.

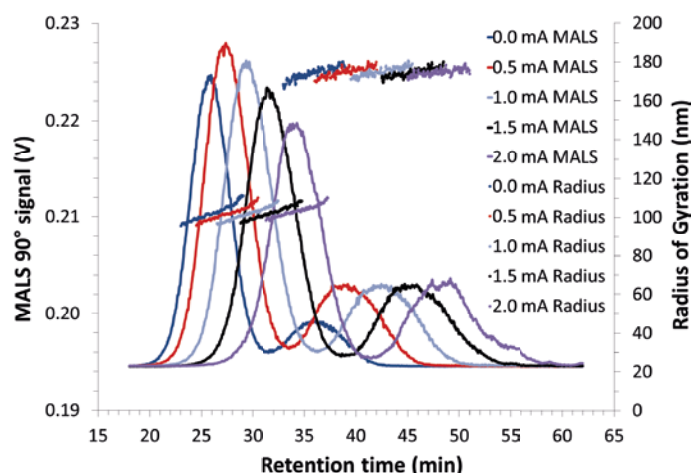


Figure 2: EAF4 separation of a bimodal silica particle sample with MALS detection. Five different electric field conditions resulted in five different retention times.

Nano-sized Silica Particles	Nominal Diameter SEM, $D_{nom, SEM}$ (nm)	Radius of Gyration SEM, $R_{g, SEM}$ (nm)	Radius of Gyration MALS, $R_{g, MALS}$ (nm)		
			at 0 mA	at 1 mA	at 2 mA
	264	102	$101.2 \pm 0.7$	$101.2 \pm 0.4$	$102.6 \pm 0.5$
	460	178	$174.6 \pm 0.6$	$174.6 \pm 0.8$	$176.1 \pm 1.6$

Table 1: Radii of gyration for both silica particles derived from SEM and EAF4-MALS with and without application of an electric field (0 mA, 1 mA and 2 mA, respectively). Radius of Gyration calculation from SEM data with the assumption of spherical particles ( $R_{g, SEM} = D_{nom, SEM} / 2 \times 0.775$ ).

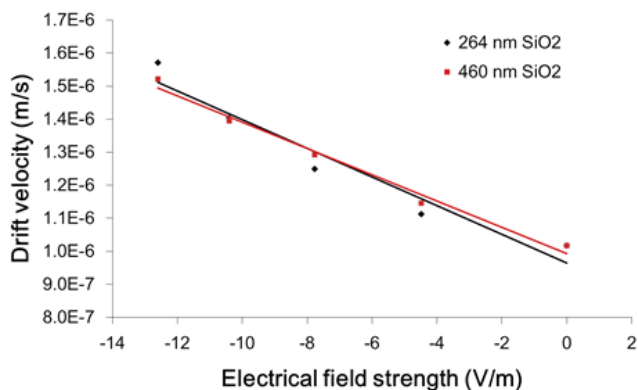


Figure 3: Drift velocity versus electric field strength plot to determine the electrophoretic mobility of the two nano-sized silica particles in the mixture.

Nano-sized Silica Particles		
Nominal Diameter, SEM (nm)	264	460
Electrophoretic Mobility, EAF4 ( $1E^{-8} \times m^2V^{-1}s^{-1}$ )	$-4.4 \pm 0.4$	$-4.2 \pm 0.3$
Zeta Potential, EAF4 (mV)	$-56.3 \pm 4.7$	$-53.7 \pm 3.2$

Table 2: Overview of the derived electrophoretic mobilities and Zeta potentials of the two size fractions in the bimodal silica sample. Zeta potentials were calculated using the Smoluchowski approximation.

## Conclusion

With increasing applications of nano-sized particles in polishing applications (e.g. in semiconductor industry) there is an increasing need for high resolution separation techniques that can not only determine the size but also give insight into the surface properties of such small particle systems. As demonstrated here, the EAF4-MALS system allows, in a single instrument, the determination of the size distribution and the electrophoretic mobility / Zeta potential of each component of a bimodal nano-sized silica particle sample thereby providing users precise information about essential physico-chemical characteristics of the CMP material.

## References

- [1] M.M. Rashad, M.M. Hessian, E.A. Abdel-Aal, K. El-Barawy, R.K. Singh, 2011, Powder Technology, 205(1-3), 149-154.
- [2] Q. He, 2018, Applied Nanoscience, 8, 163-171.